Comparison of Performances of the Various Shapes of Asymmetric Fins

Hyung Suk Kang*
(*Received April 25, 1996*)

A comparison between the heat loss of the asymmetric triangular fin and the asymmetric trapezoidal fins which have various slopes of the fin's upper lateral side is performed. The relation between the slope factor of the fin and the non-dimensional fin length for equal amount of heat loss is shown. Further, the relation between the Biot number and the non-dimensional fin length for equal amount of heat loss is given. For these analyses, a forced analytic method is used. In particular, the same equation is used for both the asymmetric triangular fin and the asymmetric trapezoidal fins just by adjusting the value of the slope factor. It is shown that this equation can also be applied to a rectangular fin with very good accuracy. The base temperature, thermal conductivity of fin's material and the heat transfer coefficient are assumed constant.

Key Words: Forced Analytic Method, Asymmetric Fin, Heat Loss, Slope Factor

Nomenclature

Bi : Biot number ($= hl/k$)
h : Coefficient of heat transfer
k : Thermal conductivity
l : Fin thickness at the base
L' : Fin length
L : Non-dimensional fin length (L'/l)
Q : Heat loss from the various shapes of asymmetric fins
Q_r : Heat loss from a rectangular fin
T : Fin temperature
T_w : Fin base temperature
T_∞ : Fin's surrounding temperature
x' : Coordinate along the fin length (base to tip)
x : Non-dimensional coordinate along the fin length (x'/l)
y' : Coordinate along the fin height
y : Non-dimensional coordinate along the fin height (y'/l)
s : Slope factor

Greek Letters

θ : Adjusted fin temperature ($T - T_\infty$)
θ_0 : Adjusted fin base temperature ($T_w - T_\infty$)
λ_n : Eigenvalues

1. Introduction

Finned surfaces are used widely in our lives. For instance, they are vital parts of the cylinder cases in the aircraft engines, the condenser tubes of a home refrigerator, heat exchangers, and many other heat transfer equipments. Much attention has been continuously directed to the fin problems. Performances of the rectangular fin (Bar-Cohen, 1979; ünal, 1985; Ju, Chou and Hsiao, 1989; Klett and Mcculloch, 1972; Look, 1988; Kang and Kim, 1994) with many different boundary conditions have been studied. There are some papers dealing with the triangular (Burmeister, 1979; Ullmann and Kalman, 1989; Kang and Look, 1993; Martin, 1982; Kang and Kim, 1994) or trapezoidal fins (Martin, 1982; Razelos, 1980) using one or two-dimensional analysis. In these

* College of Engineering, Kangwon National University

papers, the shape of a triangular fin or the shape of trapezoidal fins is symmetric. Many different methods (i. e. finite difference method, finite element method, analytic method etc.) have been used to analyze the given model of the fin. All these papers show that one equation can be applied to only one model or two (Martin, 1982). Also, many heat transfer texts (Chapman, 1984; Mills, 1995; Holman, 1981) show that the different boundary conditions are needed to analyze the performance of the different shape of the fin even in one dimensional analysis. For example, the boundary conditions for a rectangular fin are different from those for a triangular or trapezoidal fin. For this reason, each model must be analyzed separately.

This study shows that one equation for two-dimensional analysis can cover several types of fin shapes (i. e. rectangular fin, asymmetric triangular fin and asymmetric trapezoidal fins which have various slope of the upper lateral surface) just by adjusting the slope factor. Using this one equation, a comparison between the heat transfer of the asymmetric triangular fin and that of the asymmetric trapezoidal fins with different slope of the upper lateral surface is shown. Further, for arbitrary range of the non-dimensional fin length, the relation between the slope factor and the non-dimensional fin length for equal amount of heat loss is given. The variation of the temperature distributions along three different parts (i. e. bottom serface, center line and upper lateral surface) of the asymmetric trapezoidal fin is listed. Finally, for three different shapes of the fins (i. e. rectangular fin, asymmetric triangular fin and asymmetric trapezoidal fin), the relation between Biot number and the non-dimensional fin length for equal amount of heat loss is presented. For simplicity, the base temperature, the heat transfer coefficient and thermal conductivity of the fin's material are assumed constant and the condition is assumed to be steady-state.

2. Two-Dimensional Analysis

2.1 Analysis for asymmetric fins

The general equation for the upper lateral sides

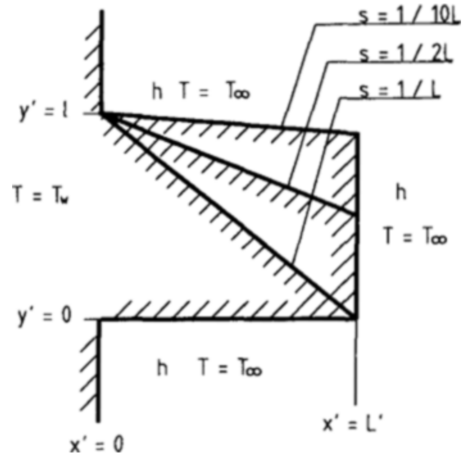

Fig. 1 Geometry of the asymmetric triangular fin and the asymmetric trapezoidal fins

of the fins shown in Fig. 1 can be written as Eq. (1):

$$y' = -s \cdot x' + l \tag{1}$$

In Eq. (1), the slope factor, s, determines the shape of the fin and the condition for $0 < s \leq l/L$ is needed. For the value of $0 < s < l/L$, the shape of the fin becomes the asymmetric trapezoidal fin and the shape of the fin becomes the asymmetric triangular fin for $s = l/L$. For various shapes of fins illustrated in Fig. 1, the governing differential equation is given by Eq. (2):

$$\frac{\partial^2 \theta}{\partial x^2} + \frac{\partial^2 \theta}{\partial y^2} = 0 \tag{2}$$

Three boundary conditions and one energy balance equation for the problem shown in Fig. 1 are

$$\theta = \theta_0 \qquad \text{at } x = 0,\ 0 \leq y \leq 1 \tag{3}$$

$$k \cdot \frac{\partial \theta}{\partial y} - h \cdot l \cdot \theta = 0 \qquad \text{at } y = 0,\ 0 \leq x \leq L \tag{4}$$

$$k \cdot \frac{\partial \theta}{\partial x} + h \cdot l \cdot \theta = 0 \qquad \text{at } x = L,\ 0 \leq y \leq 1 - s \cdot L \tag{5}$$

$$-\int_0^1 k\left[\frac{\partial \theta}{\partial x}\right]_{x=0} dy = h \cdot l \cdot \sqrt{\frac{1}{s^2} + 1} \int_{(1-s \cdot L)}^1 \theta dy - \int_0^{(1-s \cdot L)} k\left[\frac{\partial \theta}{\partial x}\right]_{x=L} dy + \int_0^L k\left[\frac{\partial \theta}{\partial y}\right]_{y=0} dx \tag{6}$$

where $\theta = T - T_\infty$, $\theta_0 = T_w - T_\infty$, $L = \frac{L'}{l}$, $x = \frac{x'}{l}$ and $y = \frac{y'}{l}$

Equation (3) represents the constant fin base temperature and Eq. (4) indicates that the heat transfer by conduction is equal to that by convection at the fin bottom. Equation (5) means the heat transfer by conduction is equal to that by convection at the fin tip. Finally Eq. (6) represents the condition that the energy into the fin at the base must escape the fin by convection from the side of the fin surface and by conduction from the fin tip and fin bottom. By solving Eq. (2) with three boundary conditions and one energy balance equation listed as Eqs. (3) through Eq. (6), the temperature profile can be obtained by usual separation of variables procedure. The result is

$$\theta=\sum_{n=1}^{\infty}\theta_0\cdot N_n\cdot f_n(x)\cdot f_n(y) \tag{7}$$

where

$$N_n=\frac{4[\lambda_n\cdot\sin(\lambda_n)+Bi\cdot\{1-\cos(\lambda_n)\}]}{AA_n+Bi^2\cdot\left\{2-\dfrac{\sin(2\lambda_n)}{\lambda_n}\right\}} \tag{8}$$

$$f_n(x)=\cosh(\lambda_n x)-\frac{1}{BB_n}\cdot\sinh(\lambda_n x) \tag{9}$$

$$f_n(y)=\cos(\lambda_n y)+\frac{Bi}{\lambda_n}\cdot\sin(\lambda_n y) \tag{10}$$

where

$$AA_n=2\lambda_n^2+\lambda_n\cdot\sin(2\lambda_n)+2Bi\cdot\{1-\cos(2\lambda_n)\} \tag{11}$$

$$BB_n=\frac{\lambda_n+Bi\cdot\tanh(\lambda_n L)}{\lambda_n\cdot\tanh(\lambda_n L)+Bi} \tag{12}$$

$$=\frac{CC_n\cdot(DD_n-EE_n+FF_n)+GG_n\cdot\cosh(\lambda_n L)+HH_n}{CC_n\cdot(II_n+JJ_n+KK_n)-GG_n\cdot\sinh(\lambda_n L)} \tag{13}$$

CC_n through II_n shown in Eq. (13) are given by Eqs. (14) through (22).

$$CC_n=\frac{Bi}{\lambda_n^2\cdot\sqrt{(1+s^2)}} \tag{14}$$

$$DD_n=\lambda_n\cdot\cos(\lambda_n)+Bi\cdot\sin(\lambda_n) \tag{15}$$

$$EE_n=\{\lambda_n\cdot\cosh(\lambda_n L)+s\cdot Bi\cdot\sinh(\lambda_n L)\}\cdot\cos\{\lambda_n(1-sL)\} \tag{16}$$

$$FF_n=\{s\cdot\lambda_n\cdot\sinh(\lambda_n L)-Bi\cdot\cosh(\lambda_n L)\}\cdot\sin\{\lambda_n(1-sL)\} \tag{17}$$

$$GG_n=\sin\{\lambda_n(1-sL)\}-\frac{Bi}{\lambda_n}\cdot\cos\{\lambda_n(1-sL)\} \tag{18}$$

$$HH_n=\frac{Bi}{\lambda_n}\cos(\lambda_n)-\sin(\lambda_n) \tag{19}$$

$$II_n=s\cdot\{\lambda_n\cdot\sin(\lambda_n)-Bi\cdot\cos(\lambda_n)\} \tag{20}$$

$$JJ_n=\{\lambda_n\cdot\sinh(\lambda_n L)+s\cdot Bi\cdot\cosh(\lambda_n L)\}\cdot\cos\{\lambda_n(1-sL)\} \tag{21}$$

$$KK_n=\{Bi\cdot\sinh(\lambda_n L)-s\cdot\lambda_n\cdot\cosh(\lambda_n L)\}\cdot\sin\{\lambda_n(1-sL)\} \tag{22}$$

where $Bi=\dfrac{hl}{k}$

Finally the value of the heat loss from the asymmetric fins shown in Fig. 1 can be obtained by Eq. (24):

$$Q=\int_0^1\left[-k\frac{\partial\theta}{\partial x}\right]_{x=0}dy \tag{23}$$

$$=-k\theta_0\sum_{n=1}^{\infty}\left[\sin(\lambda_n)+\frac{Bi}{\lambda_n}\cdot\{1-\cos(\lambda_n)\}\right]\cdot AA_n\cdot N_n \tag{24}$$

To obtain the value of eigenvalues, a forced analytic method (Kang and Look, 1993; Kang and Kim, 1994) is used. In this forced analytic method, the eigenvalue, λ_1, is calculated using Eqs. (12) and (13); then the rest eigenvalues, λ_n ($n=2, 3, 4, \cdots$), are obtained from Eq. (26). Algebraic manipulation of Eq. (25) produces Eq. (26). The direct application of orthogonality principle used in the separation of variables method produces Eq. (25):

$$\int_0^1\cos(\lambda_1 y)\cos(\lambda_n y)\,dy=0 \tag{25}$$

$$\lambda_n=(2\lambda_1+\lambda_n)-2(\lambda_1+\lambda_n)\frac{\tan(\lambda_n)}{\tan(\lambda_1)+\tan(\lambda_n)} \tag{26}$$

2.2 Analysis for a rectangular fin

In order to illustrate that Eqs. (7) and (24) also can be used to predict the performance of a rectangular fin with good accuracy, analysis for a rectangular fin is provided separately. Governing differential equation and three boundary conditions are the same as those for the asymmetric fins except that energy balance Eq. (6) is replaced by the boundary condition for the fin top. This boundary condition for the fin top is written as Eq. (27):

$$\frac{\partial\theta}{\partial y}+Bi\cdot\theta=0\quad\text{at } y=1,\quad 0\le x\le L \tag{27}$$

In particular, it must be noted that the value of s in Eq. (5) is zero for a rectangular fin analysis. Then, the temperature profile for a rectangular fin can be calculated by Eq. (28):

$$\theta = \sum_{n=1}^{\infty} \theta_0 \cdot N_n \cdot g_n(x) \cdot g_n(y) \tag{28}$$

where

$$g_n(x) = \cosh(\lambda_n x) - \frac{\lambda_n \cdot \tanh(\lambda_n L) + Bi}{\lambda_n + Bi \cdot \tan(\lambda_n L)} \cdot \sinh(\lambda_n x) \tag{29}$$

$$g_n(y) = \cos(\lambda_n y) + LL_n \cdot \sin(\lambda_n y) \tag{30}$$

where

$$LL_n = \frac{Bi}{\lambda_n} \tag{31}$$

$$= \frac{\lambda_n \cdot \sin(\lambda_n) - Bi \cdot \cos(\lambda_n)}{\lambda_n \cdot \cos(\lambda_n) + Bi \cdot \sin(\lambda_n)} \tag{32}$$

Finally the value of the heat loss from a rectangular fin can be obtained by Eq. (34):

$$Q = \int_0^1 \left[-k \frac{\partial \theta}{\partial x} \right]_{x=0} dy \tag{33}$$

$$= k\theta_0 \sum_{n=1}^{\infty} [\sin(\lambda_n) + LL_n \cdot \{1 - \cos(\lambda_n)\}] \cdot \frac{\lambda_n \cdot \tanh(\lambda_n L) + Bi}{\lambda_n + Bi \cdot \tanh(\lambda_n L)} \cdot N_n \tag{34}$$

3. Numerical Results and Discussions

Figure 2 represents the variation of the non-dimensional heat loss from the asymmetric fins as the value of Biot number varies from 0.01 to 0.1 for the non-dimensional fin length, $L=1$ in the case of the slope factor, $s=1/L$, $1/2L$, $1/4L$ and $1/10L$. The shape of the fin becomes a triangular fin for $s=1/L$. For $s=1/2L$, the shape of the fin becomes an asymmetric trapezoidal fin, and the height of the fin tip is a half of the height of the fin base. The non-dimensional heat loss increases linearly as Biot number increases for all four values of s. On the whole, in the case of $L=1$, the heat loss decreases as s increases. It means that the heat loss is the least for the asymmetric triangular fin, and that the heat loss increases as the slope of the fin's side of the trapezoidal fin decreases. Results for the same condition as in Fig. 2 except that $L=10$ are presented in Fig. 3. In this figure, the non-dimensional heat loss increases parabolically as Biot number increases. It can be

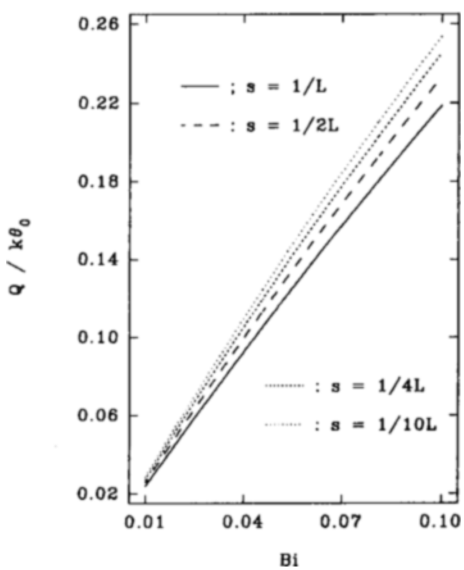

Fig. 2 Heat loss versus Biot number for $L=1$

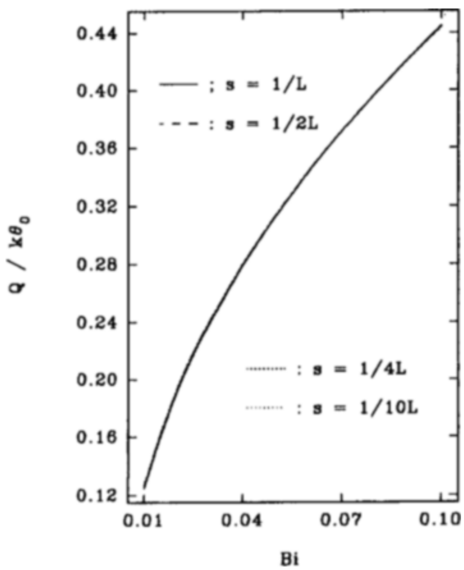

Fig. 3 Heat loss versus Biot number for $L=10$

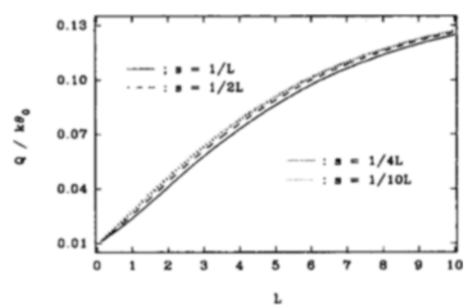

Fig. 4 Heat loss versus the non-dimensional fin length for $Bi=0.01$

noted that the values of the non-dimensional heat loss are almost the same for the given values of s. This fact explains that the amount of the heat loss can be regarded as independent upon the shape of the fin for long fin.

Figure 4 shows that the variation of the non-dimensional heat loss as a function of the non-dimensional fin length for various values of s in the case of $Bi=0.01$. The heat loss for all the values of s increases as the non-dimensional fin length increases. It is also shown that the amount of the heat loss becomes larger as the value of s decreases for a given range of the non-dimensional fin length. Figure 5 depicts the same type of information as was presented in Fig. 4 but for $Bi=0.1$.Comparing this with the case of $Bi=0.01$, the trend of the variation are similar to the $Bi=0.01$ case, but most notable point in this figure is that the heat loss becomes almost the same for all values of s as the value of L is over 7.

Table 1 lists the variation of the non-dimensional temperature along each part of the asymmetric fin in the case of $L=1$ and 10 for $s=1/2L$. In the case of $L=1$, the value of the non-dimensional temperature along the bottom surface is the lowest and that along the center line is the highest until $x=0.6$ but the non-dimensional temperature along the upper lateral surface is larger than that along the center line at $x=0.8$ for both $Bi=0.01$ and 0.1.In the case of $L=10$, the value of the non-dimensional temperature along the bottom surface is the lowest and that along the center line is the highest except $x=10$ for both $Bi=0.01$ and 0.1.

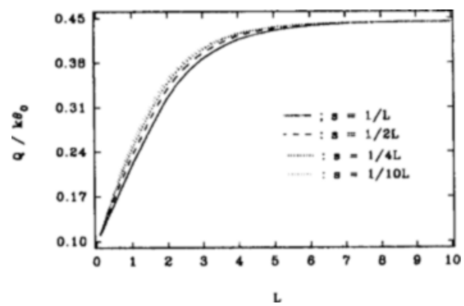

Fig. 5 Heat loss versus the non-dimensional fin length for $Bi=0.1$

Table 1 The variation of the non-dimensional temperature along each part of the asymmetric fin

	θ/θ_0 for $s=1/2L$					
	Along the bottom surface	Along the center line	Along the upper lateral surface	Along the bottom surface	Along the center line	Along the upper lateral surface
$L=1$	$Bi=0.01$			$Bi=0.1$		
$x=0.2$	0.993541	0.995590	0.995088	0.941212	0.960847	0.956141
$x=0.4$	0.988967	0.991552	0.991299	0.901587	0.925045	0.922448
$x=0.6$	0.985269	0.988055	0.988029	0.869980	0.894220	0.893856
$x=0.8$	0.982296	0.985133	0.985210	0.844787	0.868890	0.869447
$x=1.0$	0.980003	0.982848	0.982848	0.825444	0.849139	0.849139
$L=10$	$Bi=0.01$			$Bi=0.1$		
$x=2$	0.782596	0.784558	0.783377	0.404786	0.414923	0.408352
$x=4$	0.628745	0.630343	0.629817	0.166941	0.171120	0.169590
$x=6$	0.524644	0.525977	0.525788	0.069705	0.071450	0.071164
$x=8$	0.462033	0.463207	0.463169	0.031179	0.031960	0.031927
$x=10$	0.435960	0.437068	0.437068	0.018914	0.019387	0.019387

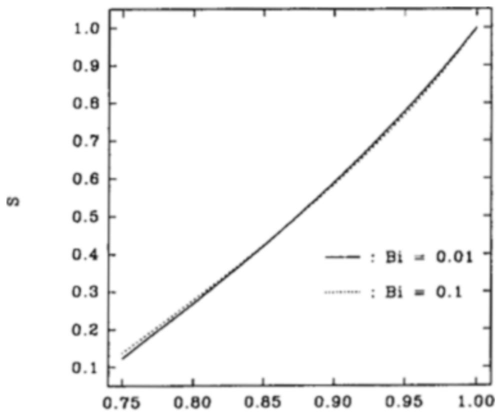

Fig. 6 Relation between the slope factor and the non-dimensional fin length for equal amount of heat loss based on the value of $s=1, L=1$

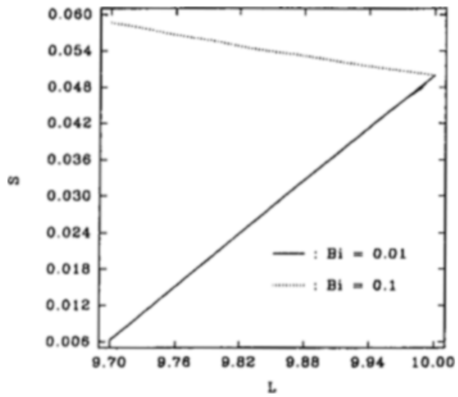

Fig. 7 Relation between the slope factor and the non-dimensional fin length for equal amount of heat loss based on the value of $s=0.05$, $L=10$

Figure 6 shows the relation between the slope factor and the non-dimensional fin length for equal amount of heat loss based on the values of $s=1.0$, $L=1.0$ for $Bi=0.01$, and $Bi=0.1$.In this figure '$L=1.0$ and $s=1.0$' describes that the shape of the fin is a triangular fin, and the non-dimensional fin length is 1. The value of s increases as L increases for both $Bi=0.01$ and $Bi=0.1$.It is also shown that the curves depict the same trend and the slope of the curve for $Bi=0.01$ case is slightly larger than the slope of the curve for $Bi=0.1$ case. Figure 7 is the same case as Fig. 6 but the based values for equal amount of heat loss are $s=0.05$, $L=10$. All the values of s and L in Fig. 7 are for the trapezoidal fins. The trend of the curve for $Bi=0.01$ in Fig. 7 is somewhat similar to that shown in Fig. 6 but the difference is such that, for the long fin, s increases linearly as L increases. In the case of $Bi=0.1$, the slope factor decreases linearly as L increases and it explains that the heat loss from a rectangular fin is less than that from the asymmetric trapezoidal fin when the non-dimensional fin length is long ($L=10$).

Table 2 lists the percent change in the heat loss for small values of the slope factors (i.e.$s \leq 1/100L$) relative to that from the rectangular fin for $L=1$ and $L=10$ in each case of $Bi=0.01$, 0.05 and

Table 2 Percent change in the heat loss ($(Q_r-Q)/Q_r$) for several values of s relative to that from the rectangular fin

Bi \ s	1/100L	1/1000L	1/10000L
		$L=1$	
0.01	0.3216	0.0305	0.0034
0.05	0.2956	0.0294	0.0029
0.1	0.2651	0.0269	0.0027
		$L=10$	
0.01	0.0220	0.0031	0.0016
0.05	0.0022	0.0003	0.0000
0.1	−0.0032	−0.0002	0.0000

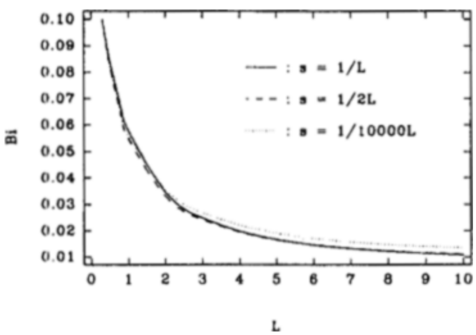

Fig. 8 Relation between Biot number and the non-dimensional fin length for equal amount of heat loss based on the value of $Bi=0.1$, $L=0.3$

0.1. The value of the heat loss from a rectangular fin as the reference value is calculated by Eq. (34). As shown in Table 2, the value of percent change decreases as s decreases for given values of Biot number and the non-dimensional fin length. Table 2 represents that Eq. (24), which is applied to the triangular and trapezoidal fins, also can be applied to a rectangular fin with less than 0.004 % relative error just by substitution of small values of s (i.e. $s \leq 1/10000L$) for the given range of Biot number and the non-dimensional fin length.

Finally Fig. 8 presents the relation between the Biot number and the non-dimensional fin length for equal amount of heat loss based on the value of $Bi=0.1$, $L=0.3$ for each three values of s. In Fig. 8, the shape of the fin is the asymmetric triangular fin for $s=1/L$, an asymmetric trapezoidal fin for $s=1/2L$ and an approximated rectangular fin with less than 0.004 % relative error for $s=1/10000L$. The value of Bi decreases rapidly as L varies from 0.3 to 2 and decreases slowly as L increases from 2 to 10. It can be noted that the values of Bi for both $s=1/L$ and $s=1/2L$ are almost the same when the value of L is larger than 5. On the whole, the trends of the curves for given values of s are similar.

4. Conclusions

From this two-dimensional analysis, the following conclusions can be drawn, and used for an appropriate design of fins.

Firstly, for the values of the non-dimensional fin length less than 6 approximately, the heat loss decreases as the slope factor increases for the range of $0.01 \leq Bi \leq 0.1$. It means that the heat loss is the least when the shape of the fin is triangular, and that the heat loss increases as the slope of the upper lateral surface of a asymmetric trapezoidal fin decreases. Secondly, for $Bi=0.1$, the amount of the heat loss can be regarded as independent on the shapes of fins when the value of L is larger than 6. Thirdly, it is shown that the value of temperature distribution of a asymmetric fin is the lowest along the bottom surface. Fourthly, the same equation can be used for the analysis of a rectangular fin with less than 0.004 % relative error as well as for that of asymmetric triangular and trapezoidal fins just by substitution of the appropriate values of the slope factor. Fifthly, the trends of curves for the relation between the slope factor and the non-dimensional fin length for the equal amount of heat loss for $Bi=0.01$ are similar to that for $Bi=0.1$ in the case of the short fin (i.e. $0.75 \leqq L \leqq 1$) while they show opposite trend, in the case of the long fin (i.e. $9.7 \leqq L \leqq 10$). Finally, the trends of curves for the relation between the Biot number and the non-dimensional fin length for the equal amount of heat loss are similar for any shapes of fins (i.e. rectangular, asymmetric triangular, and asymmetric trapezoidal fins).

References

Bar-Cohen A., 1979, "Fin Thickness for an Optimized Natural Convection Array of Rectangular Fins," *ASME Journal of Heat Transfer*, Vol. 101, pp. 564~566.

Burmeister, L. C., 1979, "Triangular Fin Performance by the Heat Balance Integral Method," *ASME Journal of Heat Transfer*, Vol. 101, pp. 562~564.

Chapman, A. J., 1984, *Heat Transfer*, Macmillan Publishing Company, New York; Collier Macmillan Publishers, London.

Holman, J. P., 1981, *Heat Transfer*, McGraw-Hill, Inc.

Ju, Y. H., Chou, Y. S. and Hsiao, C. C., 1989, "A New Approach to the Transient Conduction in 2-D Rectangular Fin," *Int. J. Heat Mass Transfer*, Vol. 32, No. 9, pp. 1657～1661.

Kang, H. S. and Kim, S. J., 1994, "Effect of Asymmetric Root Temperature on the Heat Loss from a Rectangular Fin under Unequal Surrounding Heat Convection Coefficient," *J. of KSME.*, Vol. 18, No. 6, pp. 1567～1571.

Kang, H. S. and Look, Jr., D. C., 1993, "A Forced Analytic Scheme Applied to a Two Dimensional Fin: An Unsuccessful Venture," *AIAA* 93～2854.

Kang, H. S. and Kim, S. J., 1994, "Errors in the Triangular Fin Analysis under Assuming the Fin Tip is Insulated," *J. of KSME.*, Vol. 18, No. 7, pp. 1783～1788.

Klett, D. E. and Mcculloch, J. W., 1972, "The Effect of Thermal Conductivity and Base-Temperature Depression on Fin Effectiveness," *Journal of Heat Transfer, Trans. ASME*, Aug., pp. 333～334.

Look, Jr., D. C., 1988, "2-D Fin Performance: Bi(top) >Bi(bottom)," *ASME Journal of Heat Transfer*, Vol. 111, pp. 780～782.

Martin Crawford, "Heat Transfer in Trapezoidal Straight Fins with a Periodically Varying Base Temperature," *ASME, 82-WA/HT-41.*

Mills, A. F., 1995, *Basic Heat and Mass Transfer*, IRWIN, Chicago.

Razelos, P. and Imre, K., 1980, "The Optimum Dimensions of Circular Fins with Variable Thermal Parameters," *ASME Journal of Heat Transfer*, Vol. 102, Aug., pp. 420～425.

Ullmann, A. and Kalman, H., 1989, "Efficiency and Optimized Dimensions of Annular Fins of Different Cross-Section Shapes," *Int. J. Heat Mass Transfer*, Vol. 32, No. 6, pp. 1105～1110.

ÜNAL, H. S., 1985, "Determination of the Temperature Distribution in an Extended Surface with a Non-Uniform Heat Transfer Coefficient," *Int. J. Heat Mass Transfer*, Vol. 28, No. 12, pp. 2279～2284.